Electrohydrodynamic ion emission from molten lithium nitrate

J. A. Panitz,[a] A. L. Pregenzer, and R. A. Gerber
Sandia National Laboratories, Albuquerque, New Mexico 87185

(Received 13 June 1988; accepted 10 September 1988)

Positive ions have been generated at the surface of molten lithium nitrate by applying a high electrostatic field to a thin layer of the molten salt on the apex of a field emitter tip. The ion emission process is characteristic of electrohydrodynamic ion formation, usually observed when a high electric field is applied to the surface of a liquid metal or alloy. With molten lithium nitrate, a single emission site appears at threshold. The divergence of the ion beam is several degrees. At higher field strengths multiple emission sites are observed. An ion species at $m/e = 76$ amu dominates the mass spectrum at all field strengths. This species is identified as a cluster ion $(LiNO_3)Li^+$. At low source temperatures, $(LiNO_3)_2Li^+$ is also observed. Despite the low ionization potential of lithium (5.4 eV), Li^+ accounts for $<8\%$ of the total ion current generated by the source under all operating conditions. Multiply charged lithium is not detected in the mass spectra, suggesting the electric field at the Taylor cone apex is not sufficient to field-ionize singly charged species by a postionization process.

I. INTRODUCTION

The choice of lithium as the accelerating species in the Particle Beam Fusion Accelerator II (PBFA II) at Sandia National Laboratories has made the development of a suitable lithium-ion source one of the highest priority areas in the light-ion, inertial confinement fusion (ICF) research program.[1] Research efforts are directed toward laser produced sources, lithium guns, and electrohydrodynamically driven liquid-lithium sources. Electrohydrodynamic (EHD) ion emission provides a conceptually simple process for generating an intense beam of positive ions in pulsed-power fusion accelerators. The EHD process is operationally attractive, because it uses an intrinsic characteristic of these machines (i.e., a high electric field at the anode surface) to generate an ion beam. The only requirements are the presence of a suitable liquid at the anode surface and a voltage pulse to generate the required field strength for a sufficient length of time.

An ICF ion source must produce ions uniformly on a nanosecond time scale. To deliver sufficient power (~ 100 TW/cm^2) to ignite the target, the ion current density at the anode must be of the order of 5 kA/cm^2, over an area of ~ 800 cm^2. Theory suggests that an electrohydrodynamically driven liquid-lithium ion source can meet these criteria.[2] When a liquid is exposed to an electric field that exceeds a critical value, competition between surface tension and the electric field stress produces an electrohydrodynamic instability on the liquid surface. For a perfectly uniform electric field, theory predicts that the surface will erupt into an array of uniformly spaced cusps, on a time scale and with a wavelength that are determined by the magnitude of the initial-applied electric field.[3] When the initial value of the applied field exceeds 10 MV/cm, cusps should form in <3 ns and have a characteristic spacing of <0.5 μm. At the apex of each cusp, the electric field will be greatly enhanced. When the enhanced field exceeds a value of ~ 100 MV/cm, ions will form by field evaporation of the liquid surface. If each cusp emits ~ 15 μA of ion current, the current density at the anode surface will exceed 5 kA/cm^2.

To reach the electric field strength required for EHD ion emission in a laboratory-scale experiment, we use a field emitter tip as a substrate, and initiate EHD ion emission from its apex.[4] To a very good approximation, the electric field at the apex of a field emitter tip is given by V/kR, where V is the voltage applied between the tip and a counter-electrode (separated by a distance D), R is the radius of curvature of the tip apex, and $k = 0.5 \ln(R/D)$, ~ 5 is a proportionality constant whose exact form depends on the electrode geometry.[5] Typically, $R \sim 200$ nm and $D \sim 10$ cm, producing an electric field of 10 to 100 MV/cm at the tip apex, at applied voltages of 1 to 10 kV. During the EHD process, Taylor cones are formed at the tip apex from a thin layer of liquid that coats its surface.[6] Field enhancement at the apex of a Taylor cone further decreases the tip voltage required to observe ion emission. The field enhancement at the emission site is unknown, because the actual shape of the Taylor cone at its apex cannot be measured.

In this paper we discuss the design and the operating characteristics of a field emitter tip coated with molten lithium nitrate, operating as a steady-state EHD ion source. We report the first observation of EHD ion emission from molten lithium nitrate and the first measurements of the divergence, the spatial distribution, and the mass spectra of the source. Lithium nitrate is an attractive material for EHD lithium ion production in PBFA II. It melts at a relatively low temperature (~ 260 °C) and, unlike lithium metal, lithium nitrate can be handled safely and used without fear of oxidation in poor vacuum conditions. Steady-state operation has allowed us to optimize the emission characteristics of the source in preparation for a study of EHD emission under pulsed-field conditions comparable to those encountered in PBFA II.

II. ION SOURCE

A field emitter EHD ion source was constructed from stainless-steel wire (type 302, 0.2 mm in diameter) and from 25-μ-thick, type 302 stainless-steel foil. The foil was fabricated into a ribbon ~ 6 mm wide, and ~ 25 mm long. A hole,

 0734-2101/89/010064-05$01.00

0.3 mm in diameter, was photoetched in the center of the ribbon. A 1-cm length of wire, bent at a right angle (~9 mm from one end), was passed through the hole. The short end of the wire was secured to the ribbon by a spot weld. The ribbon was formed into a semicircular loop ~4 mm in diameter and spot welded at each end to one pin of a commercial, two-pin header.[7] The header assembly was immersed in a commercial electropolishing solution, polished at several volts dc for ~1 min, and rinsed in distilled water.[8] The long end of the wire protruding through the hole in the ribbon was returned to the solution and polished until a tip was formed, ~1 mm from the surface of the ribbon. Figure 1 is a scanning electron microscope (SEM) image of the tip and the ribbon of a completed ion source. The micrograph was taken after several hours of operation (note the lithium nitrate crystals on the surface of the ribbon).

Molten lithium nitrate is highly corrosive and readily attacks most materials at temperatures above 300 °C. Stainless steel was chosen for the tip and ribbon, because it seemed desirable to study EHD ion emission from the same substrate material used for anode construction in PBFA II. Field emitter tips made of stainless steel were able to resist exposure to molten lithium nitrate for an extended period of time. Figure 2 shows the apex of a typical stainless-steel tip after exposure to molten lithium nitrate for several hours at 300 °C. Although the shape of the tip apex is clearly delineated, the morphology of the stainless-steel substrate is probably masked by a coating of lithium nitrate, since no attempt was made to clean the tip prior to SEM imaging. Several ion sources were constructed with tungsten tips electrochemically etched in 1 *N* NaOH at ~5 V(ac).[9] Figure 3 shows a tungsten tip after it was exposed to molten lithium nitrate for several hours. The smoothly etched tip apex has corroded away, leaving a jagged, unusable end-form at the end of the tip wire.

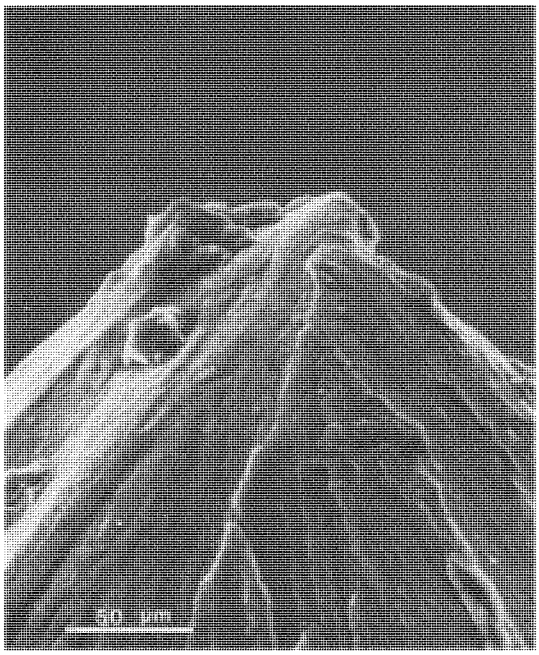

FIG. 2. A scanning electron micrograph showing the apex region of a type 302 stainless-steel, field emitter tip. The tip was exposed to molten lithium nitrate for a few hours prior to imaging.

III. WETTING CONSIDERATIONS

Two conditions must be satisfied to insure stable EHD ion emission from the apex of a field emitter tip coated with molten lithium nitrate: (i) the tip must maintain a stable morphology, and (ii) the surface of the tip must be uniformly wetted by the molten salt to insure a reliable mass flow along its surface, from reservoir to apex. A reservoir of molten lithium nitrate must be provided close to the tip apex to

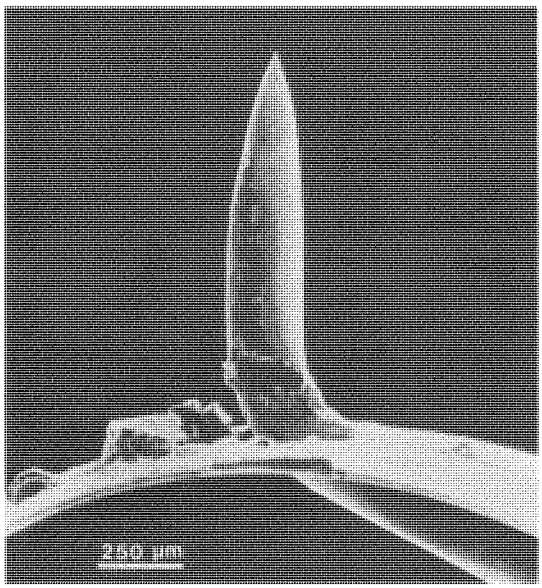

FIG. 1. A scanning electron micrograph showing the tip and ribbon end of a field emitter, EHD ion source. Lithium nitrate crystals can be seen on the surface of the ribbon.

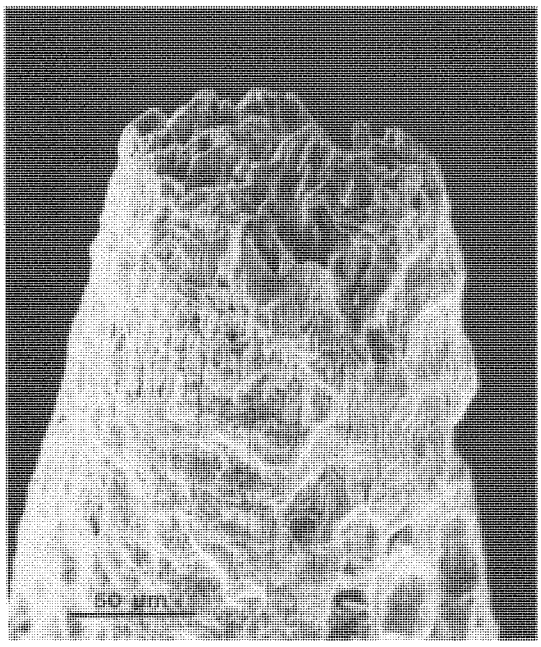

FIG. 3. A scanning electron micrograph showing the apex region of a tungsten field emitter tip. The tip was exposed to molten lithium nitrate for several hours prior to imaging.

insure the molten salt lost by evaporation from the tip surface is rapidly replaced.

Molten lithium nitrate will wet untreated type 302 stainless steel in air or in vacuum at 300 °C, but uniform wetting is difficult to achieve. To insure complete and reliable wetting of the surface, a two-step protocol was developed. First, the ribbon and the tip were heated to ~600 °C in vacuum for several minutes by passing ~3 A through the ribbon. After cooling the tip and the loop to room temperature, they were immersed in molten lithium nitrate (at ~300 °C) without breaking vacuum. The success of this procedure can be explained by noting the surface of stainless steel is depleted of chromium when it is heated to elevated temperatures in vacuum.[10] When the chromium-depleted surface is exposed to molten lithium nitrate in vacuum, the surface readily oxidizes and wets uniformly. If heat-treated stainless steel is exposed to air and is immersed into molten lithium nitrate (in air or in vacuum), the wetting process will not be effective, and the surface will not wet uniformly.

A small, turbomolecular-pumped vacuum chamber was assembled for the heat treatment and vacuum wetting procedure. Lithium nitrate was loaded in air onto a small coil of platinum wire by immersing the coil into a crucible of molten lithium nitrate that was heated in a small furnace to 300 °C. After several immersions, ~20 μL of molten lithium nitrate was retained on the coil by surface tension forces. The coil was removed from the furnace, cooled, and placed (with its charge of solidified lithium nitrate) in the vacuum chamber. A source assembly was mounted on the end of a linear manipulator and placed in the vacuum chamber opposite the coil. The coil and the source assembly could be independently heated by connecting a power supply to each of them through electrical feedthroughs provided for this purpose. An optical microscope was positioned opposite a window in the chamber wall to view both the coil and the source assembly after the chamber was evacuated. Figure 4 is a photograph of the interior of the vacuum chamber taken through this microscope.

After evacuating the vacuum chamber to ~10^{-6} Torr, the loop was heated both to melt and to outgass the lithium nitrate in vacuum. After bubbling subsided, the loop was cooled, and the tip and ribbon were heated to dull red heat for several minutes. After they cooled to room temperature, the lithium nitrate was heated to its melting point (judged by the existence of a stable mixture of molten and solid lithium nitrate in the loop). Heating current was applied to the ribbon, and the tip was translated into the loop. Lithium nitrate was observed to wick along the tip wire. When the ribbon was moved closer to the loop, the lithium nitrate transferred from the coil onto the ribbon, filling the reservoir to capacity. After loading a source with lithium nitrate, the source was removed from the vacuum chamber and stored in an airtight container filled with desiccant.

IV. EHD ION EMISSION

The EHD emission characteristics of a source were observed visually during dc operation, in real time, by allowing the emitted ions to strike a microchannel plate (MCP) image intensifier placed several centimeters from the tip apex in a high-vacuum chamber. The magnification of an image on the MCP screen is ~$D/\beta R$, where D is the MCP-to-tip distance, R is the tip radius, and $\beta \sim 1.5$ is a proportionality factor that describes deviation from pure radial projection ($\beta = 1$).[9] Typical emission patterns are shown in Fig. 5 at a magnification of ~10^5. The emission pattern at threshold (defined by the onset of stable ion emission) is shown in Fig. 5(a). The ion beam has an angular divergence of several degrees. A similar divergence was measured at threshold for six other lithium nitrate sources. A distinct threshold vol-

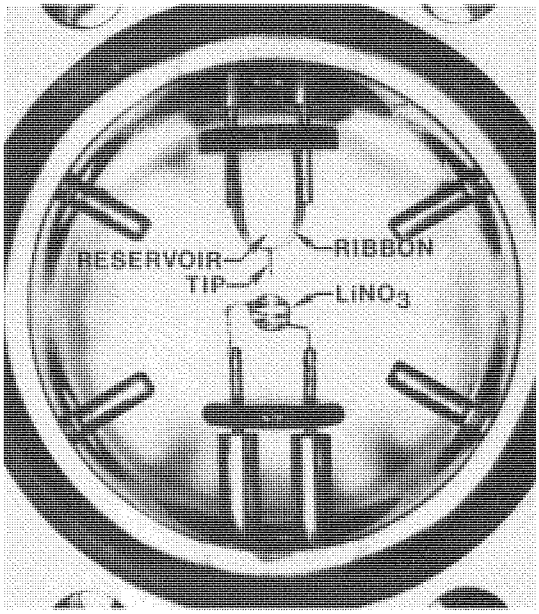

FIG. 4. The interior of a turbomolecular-pumped vacuum chamber used to wet field emitter tips with molten lithium nitrate.

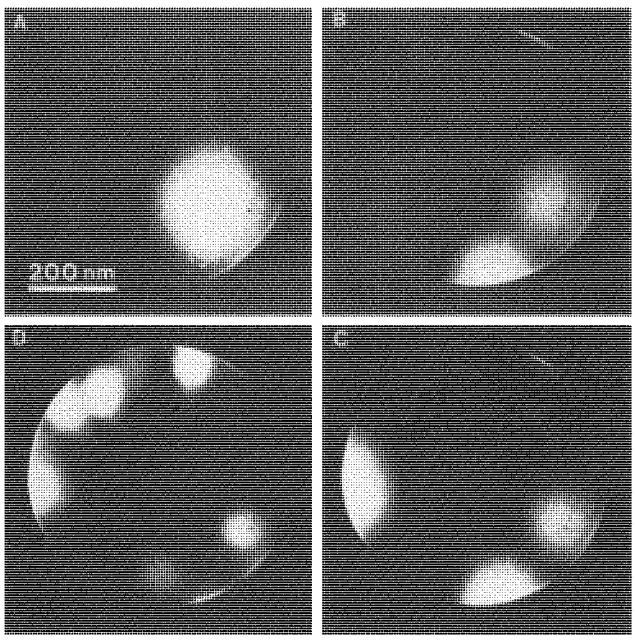

FIG. 5. EHD ion emission from molten lithium nitrate at the apex of a stainless-steel, field emitter tip. Threshold at (a) 3.0, (b) 3.5, (c) 4.0, and (d) 5.5 kV.

tage was observed with each source between 3.0 and 4.0 kV. As the tip voltage (i.e., the field strength) was increased, more emission sites appeared on the MCP phosphor screen, as shown in Figs. 5(b)–5(d). The emission current and the number of emission sites at a given field strength were very reproducible for each source examined. The emission patterns observed in this study are similar in appearance to the structureless emission patterns seen when liquid gallium EHD ion sources are operated at low emission currents.[11]

V. MASS SPECTROSCOPY

Six ribbon sources were heat treated, loaded with lithium nitrate in vacuum, and stored in desiccant-filled containers until mass spectra could be obtained. Mass spectra were measured in a single-focusing, 90° magnetic-sector mass spectrometer equipped with a Be–Cu electron multiplier detector.[12] Spectra were obtained by plotting the electron multiplier current as a function of the magnetic field strength (m/e is proportional to the square of the field strength). Figure 6(a) shows a typical mass spectrum obtained with a $LiNO_3$ EHD ion source at two reservoir temperatures. The reservoir temperature could not be directly measured. Instead, the ribbon current I_R (proportional to the reservoir temperature) was measured. The appearance of the reservoir was monitored in an optical microscope as the heater current was increased. When a mixture of solid and molten lithium nitrate was observed the temperature of the reservoir was judged to be close to the melting point of lithium nitrate. Figure 6(a) was taken at $I_R \sim 1.5$ A, close to the melting point of molten lithium nitrate. Figure 6(b), taken at $I_R \sim 2$ A, corresponds to a much higher reservoir temperature, but below the boiling point of lithium nitrate. The dominant species in the mass spectrum at all reservoir temperatures (between the melting point and the boiling point of lithium nitrate) is the cluster ion $(LiNO_3)Li^+$. At low reservoir temperatures $(LiNO_3)_2Li^+$ is observed. At higher reservoir temperatures this species is not detected. Cluster ions of this form have also been observed during field desorption of molten KCl and NaCl crystals in vacuum.[13]

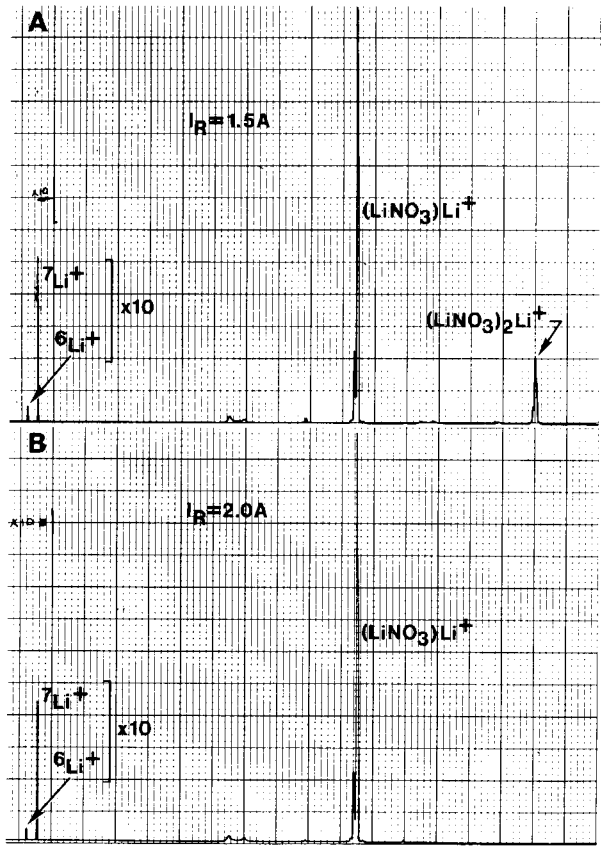

FIG. 6. Mass spectra of EHD ion emission from molten lithium nitrate at the apex of a stainless-steel, field emitter tip. Ion current is plotted as a function of magnetic field strength: (a) source 4 close to the melting point of lithium nitrate and (b) source 4 just below the boiling point of lithium nitrate.

The amplitudes of the Li^+ peaks in Fig. 6 have been magnified 10× for clarity. From a measurement of the area under each peak in the mass spectrum, we conclude the abundance of Li^+ is $<8\%$ of the integrated abundance of all other species in the mass spectra (at any reservoir temperature). Li^{2+} and Li^{3+} ions were never observed during EHD operation of these sources when molten lithium nitrate was present in the reservoir. When the reservoir was depleted of lithium nitrate, ion emission could be induced for many minutes by increasing the field strength and raising the source temperature. The mass spectra changed dramatically under these conditions. The total ion current decreased, Li^+ ions dominated the mass spectra, and a small abundance ($\sim 0.1\%$) of Li^{2+} was observed. Cluster ions disappeared from the mass spectra. The change in the emission characteristics of the source is attributed to a different mode of operation. We speculate that when the reservoir is depleted of lithium nitrate, EHD ion emission disappears and ions are generated by thermally enhanced field desorption of a lithium-rich residue from the tip surface. Li^{2+} could be produced under these conditions by a post field-ionization process, since a higher field strength is required to initiate ion emission. Post field ionization is the mechanism generally used to explain the formation of the multiply charged ions observed during field evaporation of refractory metals at high field strengths.[14] The generation of ions from a lithium-rich surface layer may be of practical interest, because it could provide a method to prepare anode surfaces for PBFA II that would produce a pure Li^+ beam without the need to maintain a layer of molten material at the surface.

Figure 7(a) shows a mass spectrum obtained with another source operating at $I_R \sim 1.4$ A, close to the melting point of molten lithium nitrate. A comparison of Figs. 6(a) and 7(a) demonstrates the reproducibility of ion emission from two different sources operated at similar reservoir temperatures. Figure 7(b) shows a magnified scan through the most abundant lithium isotope peak ($^7Li^+$), taken as a function of total emission current I_T. At low emission currents ($I_T \sim 0.8\,\mu A$) the $^7Li^+$ peak is dominant. When the field at the tip apex is increased (by increasing the extraction voltage V_E), the emission current increases and a shoulder, shifted to higher masses, appears in the spectra. The amplitude of the shoulder and the peak shift increases with increasing emission current. At high emission currents ($I_T \sim 10\,\mu A$) the shoulder dominates the mass spectra. Each of

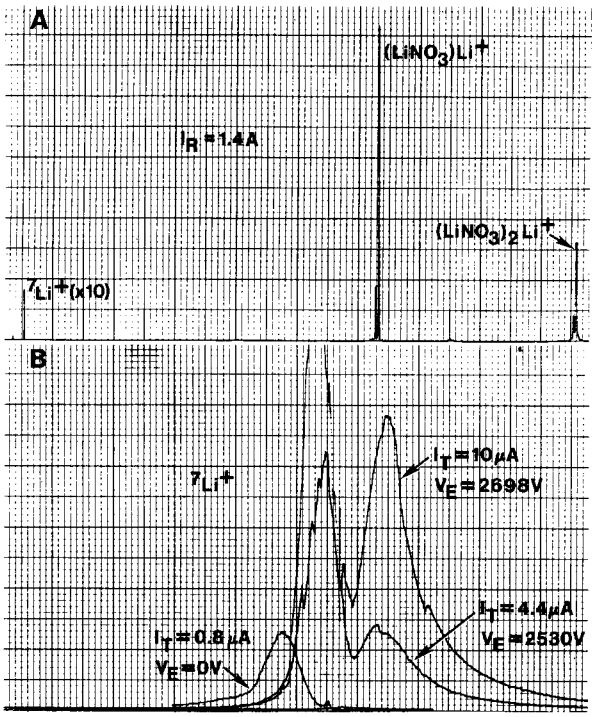

FIG. 7. Mass spectra of EHD ion emission from molten lithium nitrate at the apex of a stainless-steel, field emitter tip. Ion current is plotted as a function of magnetic field strength: (a) source 3 close to the melting point of lithium nitrate and (b) mass scan through $^7Li^+$ peak (source 3) as a function of total emission current.

the other species in the mass spectrum behaved in a similar fashion. We attribute the shoulder to ionization processes in the vicinity of the tip apex because a peak shift toward higher m/e is characteristic of ions formed at a position in space where the potential is less than the tip bias.

VI. CONCLUSIONS

Ion emission has been observed from the apex of stainless-steel field emitter tips coated with molten lithium nitrate in the presence of a high electric field. The ion formation process is interpreted as EHD ion emission, because it exhibits features that are characteristic of EHD ion emission from field emitter tips coated with liquid metals. The stability of the emission process is dependent on the stability of the tip (i.e., its resistance to corrosion) and on an uninterrupted flow of lithium nitrate along its surface. Uniform wetting of the tip surface by molten lithium nitrate is a prerequisite for optimum mass flow, and for stable ion emission.

Mass spectroscopy has revealed three characteristic features of ion emission from molten lithium nitrate EHD ion sources (operating in a dc mode, under steady-state conditions): (i) Li^+ ions comprise $<8\%$ of the total emission current, (ii) Li^{2+} and Li^{3+} ions are not present in the mass spectrum, and (iii) the dominant species in the mass spectrum at all reservoir temperatures is the cluster ion $(LiNO_3)Li^+$. The results of this study differ significantly from an earlier study of EHD ion emission from field emitter tips coated with lithium (meta)borate.[15] In that study Li^+ accounted for 78% of the total emission current, $Li_2BO_2^+$ for 18%, and Li^{2+} for 2% of the total emission current. In the present study Li^{2+} and Li^{3+} were observed only when the reservoir was depleted of lithium nitrate.

We cannot predict if the ion species observed under dc operation of the source will also be observed when the source is operated in a pulsed mode, on a nanosecond time scale. Pulsed-field experiments are planned to answer this question. Pulsed-field operation will utilize imaging atom-probe techniques for spatial diagnostics and for analysis of the ion species by time-of-flight mass spectroscopy.[16]

ACKNOWLEDGMENTS

One of us (JAP) wishes to thank Lynn Swanson of the FEI Company, and Tony Bell of the Oregon Graduate Center (OGC), for a stimulating visit to their facilities in Beaverton. The mass spectra presented in this paper were taken by Greg Schwind at OGC, and many fruitful discussions were held with OGC faculty. A special note of thanks is given to Doug Barofsky of Oregon State University, who helped to identify the cluster ion species we observed. This research was supported by the U.S. Department of Energy under Contract No. DE AC04-76-DP00789.

[a] Present address: Department of Physics, University of New Mexico, 800 Yale Boulevard NE, Albuquerque, NM 87131.

[1] J. P. VanDevender and D. L. Cook, Science **232**, 831 (1986).
[2] A. L. Pregenzer and B M. Marder, J. Appl. Phys. **60**, 3821 (1986).
[3] A. L. Pregenzer, J. Appl Phys **58**, 4509 (1985).
[4] R. Clampitt and D. K. Jefferies, Nucl. Instrum. Methods **149**, 739 (1978).
[5] R. Gomer, *Field Emission and Field Ionization* (Harvard University, Cambridge, 1961), p. 45.
[6] G. I. Taylor, Proc. R. Soc. London Ser. A **280**, 383 (1964).
[7] AEI filament base, EBTEC Corp., Energy Beam Sciences Division, Agawam, MA 01001.
[8] Electroglo 300 (electropolishing concentrate), Electroglo Co., Chicago, IL 60624.
[9] E. W. Müller and T. T. Tsong, *Field Ion Microscopy:Principles and Applications* (Elsevier, New York, 1969), p. 119.
[10] R. L. Park, J. E. Houston, and D. G. Schreiner, J. Vac. Sci. Technol. **9**, 1023 (1972).
[11] A. E. Bell, K. Rao, G. A. Schwind, and L. W. Swanson, J. Vac. Sci. Technol. B **6**, 927 (1988).
[12] Hitachi, model RMU-7; see acknowledgments.
[13] F. Okuyama, S. S. Wong, and F. W. Röllgen, Surf. Sci. **151**, L131 (1985).
[14] R. Haydock and D. R. Kingham, Phys. Rev. Lett. **44**, 1520 (1980).
[15] V. G. Dudnikov and A. L. Shabalin, Sov. Tech. Phys. Lett. **11**, 335 (1985).
[16] J. A. Panitz, in *Methods of Experimental Physics*, edited by R. L. Park and M. G. Lagally (Academic, New York, 1985), Vol. 22, p. 349–423.